

# Phenylthiophene–Dipicolinic Acid-Based Emitters with Strong Solution Blue and Solid State Green Emission

Ana de Bettencourt-Dias\* and Andrei Poloukhine

Department of Chemistry, Syracuse University, Syracuse, New York 13244-4100

Received: July 27, 2006; In Final Form: October 26, 2006

The synthesis and characterization of highly efficient blue emitting phenyl–thiophene compounds derivatized with dipicolinic acid bis(diethylamide) and dipicolinic acid diethyl ester **1**, **2**, and **3** are reported. Quantum yields were determined to be between 97% and 76% in methanol and 99% and 49% in toluene solution. The solvent dependences of the solution luminescence behavior are discussed in terms of solvent refractive index and dielectric constant as well as hydrogen-bonding capability. Luminescence is also observed in the solid state for the three compounds. A bathochromic shift in the emission wavelength is accompanied by solid-state quantum yields between 29% and 4%. HOMO and LUMO energies, in the range  $-5.55$  to  $-5.71$  eV and  $-2.20$  to  $-2.48$  eV, respectively, were determined experimentally from cyclic voltammetry and absorption spectroscopy experiments. The electrochemical characterization revealed that cyclic voltammetry can be utilized to deposit thin films of **3**. An X-ray quality single crystal of **1** was isolated. This compound crystallizes in the monoclinic space group  $P2_1/c$  with cell parameters  $a = 15.224(3)$  Å,  $b = 8.9383(18)$  Å,  $c = 17.234(3)$  Å,  $\beta = 114.36(3)^\circ$ , and  $V = 2136.4(7)$  Å<sup>3</sup>. Appreciable solid state interactions in the form of  $\pi$ – $\pi$  or S–S short contacts are not present, only weaker C–H $\cdots\pi$ . A large torsion angle of  $30.28^\circ$  between the phenyl and thiophene moieties and a small torsion angle of  $-3.37^\circ$  between the pyridine and the thiophene moieties are seen.

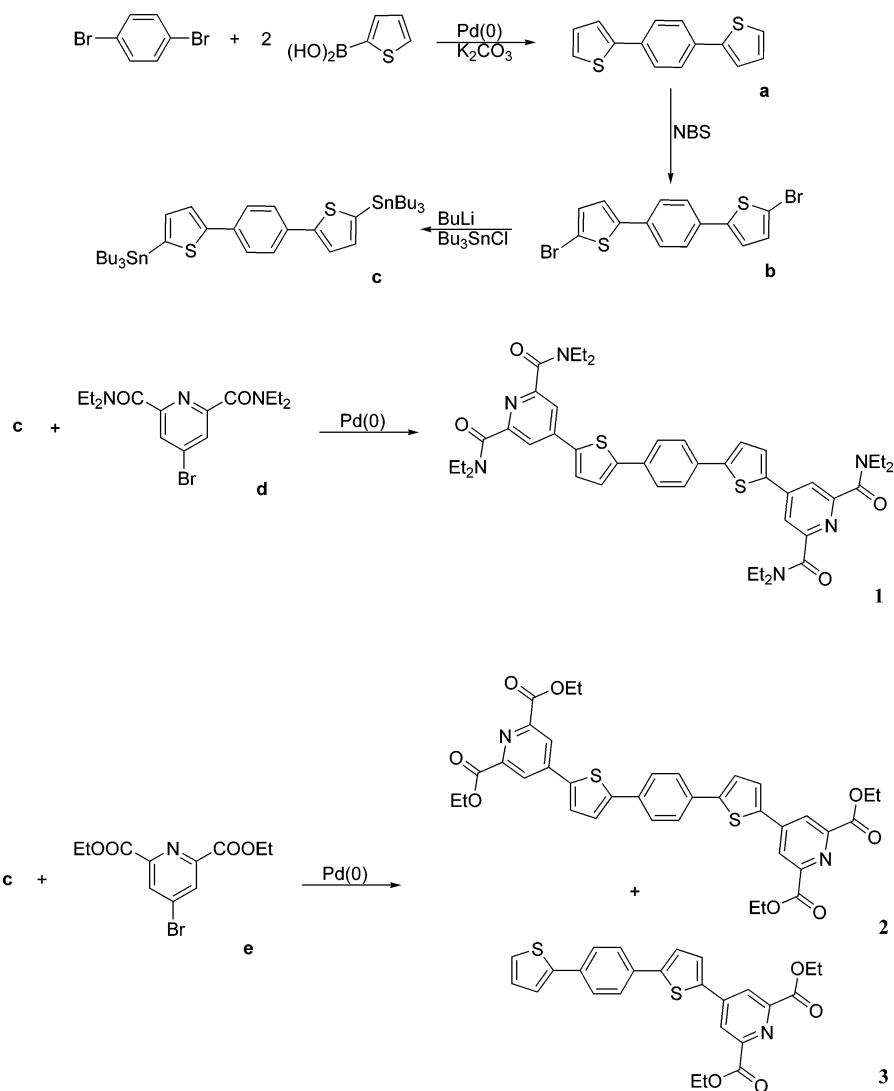
## Introduction

Since the discovery of efficient green electroluminescence of Alq<sub>3</sub> by Tang and VanSlyke,<sup>1</sup> several coordination complexes and organic molecules have been used as emitting layers in organic light-emitting diodes (OLEDs).<sup>2–6</sup> Although OLED-based displays are available commercially, much work still needs to be done to improve long-term stability and energy efficiency of the devices, particularly when considering emitting materials in the three primary colors, red, green, and blue, which are used in multicolor displays. Blue-emitting materials show shorter device lifetimes and less intense emission bands than their longer wavelength counterparts. A large component of the current research efforts in the area of multicolor OLEDs is in the area of new materials with efficient blue luminescence and long device operation times.<sup>7–17</sup> Recent work has also focused on Ln(III) ions as the emitters, due to the high color purity of the emission from these ions.<sup>18–27</sup> In our group we are interested in these ions as the emitters and have synthesized and tailored ligands for efficient luminescence.<sup>28</sup> Thiophene has been incorporated into our ligand design, to allow inclusion of Ln(III) ion complexes into polymers. However, due to the lack of electropolymerization ability of the monothiophene ligands developed,<sup>29</sup> more extended backbones are being targeted. Terthiophene, a possible backbone, has long been known as a blue emitter<sup>30</sup> and other oligothiophene derivatives have also been extensively studied as possible blue-emitting materials.<sup>31</sup> However, some functionalized oligomers show photoluminescence in the green to red region with modest quantum yields.<sup>32,33</sup> The large tendency for crystallization usually presented by short oligomers, responsible for the formation of aggregates,<sup>31</sup> and

the extended conjugation, resulting in the planarity of the oligothiophenes, are responsible for the photophysical characteristics. In fact, Gigli and co-workers observed that the introduction of methyl groups and derivatizing the central sulfur atom in quinquethiophene led to an increase in photoluminescence efficiency from 2% to 37% in the solid state due to the loss of planarity induced by the methyl groups and the de-aromatization due to the dioxide functionalization.<sup>33</sup> Chan and co-workers reported that insertion of phenyl rings in between thiophene units results in increased inter-ring torsion angles with consequent reduced conjugation and leads to hypsochromic emission shifts.<sup>34</sup> 1,4-Bis(5-phenylthiophen-2-yl)benzene, PTPTP, a simple thiophene–phenylene oligomer, described by Hotta and co-workers,<sup>35</sup> shows efficient blue solution and green solid-state luminescence and has gained attention as being representative of a new class of organic semiconductors for field-effect transistor applications.<sup>36,37</sup>

Since we are interested in developing blue emitting materials which do contain the versatile thiophene heterocycle, we have introduced a phenyl ring in between two thiophene moieties, similarly to PTPTP, to allow for disturbance of the usual stacking arrangements of oligothiophenes. Further, dipicolinic acid derivatives were added at the edges of the thiophene–phenyl–thiophene unit. These moieties act as potential sites for further functionalization of the materials with metal ions, and possible use as sensitizers for Ln(III) ion emission, or allow for derivatization with branched alkyl groups to avoid quenching of solid-state luminescence due to the formation of aggregates, as well as to improve processability.<sup>32</sup> The compounds presented here show interesting emission properties on their own and the photophysical and electrochemical characterization illustrates their potential use as blue and green emitters in LEDs.

\* Address correspondence to this author. E-mail: debetten@syr.edu. Phone: 315-443-2006. Fax: 315-443-4070.

SCHEME 1: Synthesis of Compounds **1** through **3**

## Results and Discussion

**Synthesis.** The synthesis of the target compounds **1** through **3** was easily accomplished in a few steps, detailed in Scheme 1. Precursors **a** through **c** were synthesized in high yields through modified literature procedures. The tributyltin derivative **c** was coupled under Stille conditions with the bromide of the dipicolinic acid derivative of interest, **d** or **e**. The coupling with compound **d** yielded **1** in a yield of 23%. The yield is low, especially when compared with the synthesis of the closely related PTPTP, described by Hotta and co-workers, who reported yields of approximately 90% for the final step.<sup>35</sup> However, the synthesis reported was a Grignard coupling, while here a different technique, Stille coupling, was utilized, due to the incompatibility of the Grignard conditions with substrate **d**, and the synthesis was not further optimized. In the case of the diethyl ester derivative **e**, two products formed in relatively low yields, one corresponding to the expected compound with two dipicolinato groups at the two ends of the thiophene–phenyl–thiophene unit and the other with only one dipicolinato and an unsubstituted terminal thiophene. No attempts were made thus far to synthesize the analogous monosubstituted thiophene–phenyl–thiophene dipicolinic acid bis(diethylamide), as the photophysical characterization of these molecules shows that this will likely be a less efficient blue emitter than the

bis-derivative. All three compounds were easily purified by column chromatography.

**X-ray Structure.** Compound **1** crystallized from methanol solution in the form of long pale yellow needles that could be isolated for X-ray single-crystal structure determination. Crystallographic details are summarized in Table S1 and selected bond distances and angles are available in Table S2 as Supporting Information. One-half of the molecule crystallizes in the asymmetric unit and the remainder is generated through a crystallographic inversion center at the center of the phenyl ring, as can be seen in Figure 1. Despite what we and others have observed for thiophene-containing molecules, no disorder related to free rotation along the C–C bond between thiophene and other aromatic rings is observed in this molecule.<sup>29,32,38,39</sup> The torsion angle between the thiophene and the pyridine moieties is very small at 3.37°, almost coplanar and indicative of a high degree of delocalization between the two rings. By comparison, thiophene derivatized at the 3-position with pyridine dicarboxylic acid, recently reported by our group, shows a torsion angle between the thiophene and the pyridine ring of 11.89°. <sup>29</sup> Both of these values are significantly smaller than the calculated gas-phase torsion angles of 17.27° and 25.65°, respectively. In **1** the torsion angle of 30.28° between thiophene and phenyl rings still allows for a certain degree of delocalization, but departs substantially from a coplanar arrangement. It has been reported

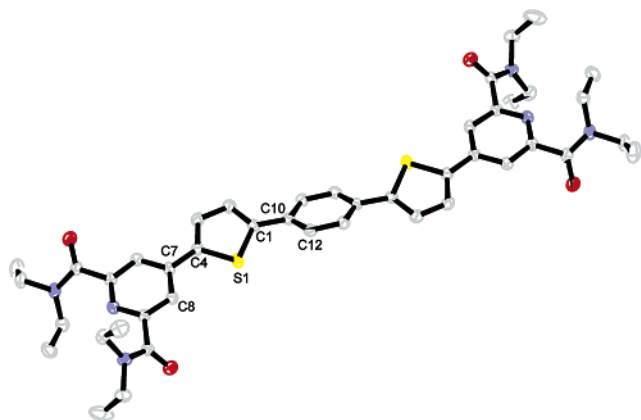


**Figure 1.** ORTEP drawing of **1**. Thermal ellipsoids are shown at 50% probability. Hydrogen atoms have been omitted for clarity. Selected torsion angles are C8–C7–C4–S1  $-3.37^\circ$  and S1–C1–C10–C12  $30.28^\circ$ .

that in oligothiophenes which are unsubstituted at the  $\beta$ -carbons the interring torsion angles are below  $1^\circ$ , with the exception of  $\alpha$ -terthiophene, with torsion angles between  $6^\circ$  and  $9^\circ$  and  $\alpha$ -quaterthiophene with torsion angles between  $3^\circ$  and  $4^\circ$ .<sup>40,41</sup> The presence of the phenyl ring between the two thiophene units leads thus to a substantial deviation from coplanarity in the central part of the molecule. This is in agreement with Gigli and co-workers who observed that the introduction of methyl groups and derivatizing the central sulfur atom in quinquethiophene led to an increase in photoluminescence efficiency from 2% to 37% in the solid state due to the loss of planarity induced by the methyl groups and the de-aromatization due to the dioxide functionalization.<sup>33</sup> Dansette and co-workers isolated 2,5-diphenylthiophene and found  $8.3^\circ$  and  $8.7^\circ$  between the terminal phenyl rings and the central thiophene.<sup>42</sup> No other thiophene–phenyl torsion rings have been reported with the thiophene substituted at the 2-position with the phenyl ring, but Ando and co-workers calculated the torsion angle of 3-phenylthiophene to be  $32^\circ$ ,<sup>43</sup> and De Almeida and co-workers estimated a torsion angle of  $41.4^\circ$  for the 3-phenylthiophene dimer.<sup>44</sup> These values, along with the experimentally found angle for compound **1**, are consistent with a low degree of  $\pi$ -delocalization between these two rings.

The unit cell of **1** contains four molecules. The packing structure of the thiophene–phenyl–thiophene backbone and the orientation of the aromatic rings with respect to one another are displayed in Figure 2a. The arrangement is reminiscent of the typical herringbone structure of oligothiophenes, with each molecule displaced by half a unit cell with respect to its immediate neighbors, coincident with the 2-fold screw axis. This arrangement, along with the lack of planarity of the individual molecules, leads to loose packing.  $\pi$ – $\pi$  stacking interactions are lacking between immediately adjacent molecules. Short contacts in the form of C–H $\cdots\pi$ , C–H $\cdots$ S, and S–S interactions determine the charge transport behavior in oligothiophenes and are therefore important in components for electroluminescent devices.<sup>29,31</sup> While short C–H $\cdots$ S contacts are absent, weak C–H $\cdots\pi$  intermolecular interactions are observed and are shown in Figure 2a. A distance of 2.87 Å is seen between the terminal methyl group C–H of a bis(diethylamide) and the pyridine ring of an adjacent molecule. A much weaker interaction between a thiophene C–H and the same pyridine ring is seen, with  $d = 3.83$  Å. By comparison, for methylated  $\alpha$ -sexithiophene a short C–H $\cdots\pi$  distance of 2.59 Å was reported.<sup>32</sup> S–S interactions,

which are often found in oligothiophene solids in the range 3.6 to 4.19 Å,<sup>40</sup> are absent in this structure, as adjacent sulfur atoms are 6.17 Å apart.

A weak hydrogen-bonding network involving the ethyl group of the amide moiety and the carbonyl oxygen of the same functional group on neighboring molecules is also present in the structure, as shown in the projection along the crystallographic  $b$ -axis in Figure 2b. We have shown previously for thiophene-functionalized benzoic acid and pyridine dicarboxylic acid derivatives that weak hydrogen bond interactions are present in the range 2.366 to 2.694 Å, which are consistent with compounds of this type.<sup>29,45</sup> O $\cdots$ H–C distances for **1** are 2.79 and 2.87 Å and indicate weaker interactions than in the previously reported compounds.

**Photophysical Characterization.** All three compounds studied here absorb in the UV, at wavelengths between 376 and 395 nm. They are also highly luminescent in the blue region of the visible spectrum. Details of the photophysical characterization are summarized in Table 1. The emission bands, shown in Figure 3, are broad and tailing and have maxima between 440 and 464 nm with quantum yields of luminescence between 96% and 76% in methanol. Some vibrational fine structure is seen in the emission band of **1**. The excitation spectra of all three compounds follow closely the absorption behavior, which results in the Stokes shift being largest for **3**. Compound **1** has the strongest and most blue-shifted emission at 440 nm, while **3** displays the lowest efficiency at the longest emission wavelength of 464 nm. Comparison of the quantum yields of **2** and **3** clearly shows that the symmetrical nature of **2** is advantageous for the emission behavior.

The emission of the compounds described in this paper was also studied in solvents with different polarities and solvation ability. In chloroform, the three compounds absorb in the range 378 to 396 nm, while the emission maxima are in the range 454 to 463 nm, with quantum yields between 36% and 80%. In the same solvent and for comparison, PTPT displays absorption and emission maxima at 430 and 453 nm, with a quantum yield of 74%.<sup>36</sup> In all solvents moderate to high luminescence was seen down to concentrations of  $10^{-7}$  to  $10^{-8}$  M. A solvent-dependent emission behavior, summarized in Table 1, is observed. The average quantum yields of emission are for **1**  $77.6 \pm 21.5\%$ , for **2**  $85.6 \pm 8.1\%$ , and for **3**  $45.8 \pm 16.1\%$ . While **2** has the highest average luminescence, **1** displays the strongest emission of all three compounds with a 99% quantum yield in toluene. These values are comparable to and among the highest seen for blue emitting organic oligomers, for which quantum yields in the range 24% to 95% have been reported.<sup>46–48</sup> The highest individual emission efficiencies are seen in toluene for the symmetrical compounds **1** and **2** and in methanol for the unsymmetrical **3**. It is seen again in these solvents that the unsymmetrical nature of **3** translates into lower efficiency of luminescence.

While both absorption and emission maxima change with the polarity of the solvent, the change is more dramatic for the emission values. The absorption maxima vary within a range of 8 and 6 nm for the individual three compounds, while the fluorescence maxima vary within ranges of 22, 32, and 52 nm for **1**, **2**, and **3**, respectively. This is consistent with the Franck–Condon excited state being structurally similar to the ground state and the emissive state showing a different geometry, more likely to experience stronger solvation in more polar solvents. Compound **3** displays the largest bathochromic shift, most likely due to its unsymmetrical nature with a nonzero dipole moment in the ground and excited state.

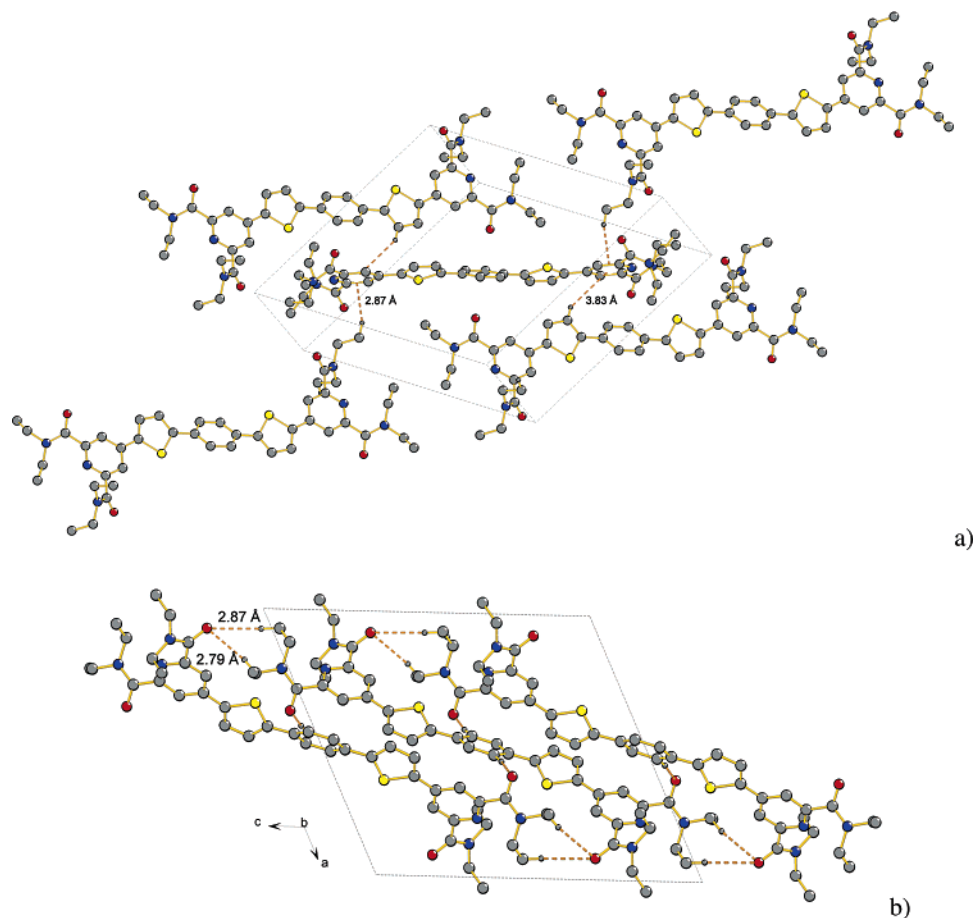


**Figure 2.** Packing diagram of **1** with selected hydrogen atoms omitted for clarity. (a) C–H... $\pi$  bonding network shown as orange segmented lines and with relevant distances (2.87 Å and 3.83 Å) indicated. (b) H-bonding network shown as segmented orange lines; view along the crystallographic *b*-axis, with relevant distances ( $d(\text{O}\cdots\text{H}) = 2.79$  and 2.87 Å) indicated.

**TABLE 1: Solvent Dependence in Terms of  $F$  and  $\mu$  of the Photophysical Properties of **1**, **2**, and **3****

compd		solvent =				
		toluene $\mu[\text{D}] = 0.375$ ; $F = -0.060$	$\text{CHCl}_3$ $\mu[\text{D}] = 1.04$ ; $F = 0.127$	$\text{CH}_2\text{Cl}_2$ $\mu[\text{D}] = 1.6$ ; $F = 0.223$	methanol $\mu[\text{D}] = 1.7$ ; $F = 0.365$	acetonitrile $\mu[\text{D}] = 3.93$ ; $F = 0.356$
<b>1</b>	$\lambda_{\text{abs}}/\text{nm}$	393	389	389	390	385
	$\lambda_{\text{ex}}/\text{nm}$	382	372	370	384	366
	$\lambda_{\text{em}}/\text{nm}$	447	458	445	440	462
	$\Phi^a$	0.99	0.58	0.89	0.96	0.46
<b>2</b>	$\lambda_{\text{abs}}/\text{nm}$	396	396	396	395	390
	$\lambda_{\text{ex}}/\text{nm}$	383	385	384	384	382
	$\lambda_{\text{em}}/\text{nm}$	447	454	454	479	468
	$\Phi^a$	0.98	0.80	0.82	0.87	0.76
<b>3</b>	$\lambda_{\text{abs}}/\text{nm}$	376	378	373	374	370
	$\lambda_{\text{ex}}/\text{nm}$	363	364	363	362	361
	$\lambda_{\text{em}}/\text{nm}$	449	463	467	501	475
	$\Phi^a$	0.49	0.36	0.34	0.44	0.34

<sup>a</sup> Absolute value at  $\lambda_{\text{exc}} = 366$  nm with  $5 \times 10^{-6}$  M quinine sulfate in 0.1 N  $\text{H}_2\text{SO}_4$  (54.6%) as the reference.

Lippert<sup>49</sup> and Mataga et al.<sup>50</sup> studied the solvation of the excited state of fluorescent molecules in detail. They concluded that in the absence of strong short-range interactions, such as hydrogen bonds between emissive solute and solvent, the magnitude of the Stokes' shift  $\Delta\bar{\nu}$  is approximately given by

$$\Delta\bar{\nu} = \bar{\nu}_a - \bar{\nu}_f \approx (\mu_e - \mu_g)^2 \times F$$

$$F = \frac{2\epsilon - 2}{2\epsilon + 1} - \frac{2n^2 - 2}{2n^2 + 1}$$

where  $\mu$  is the dipole moment of ground and excited states,  $\bar{\nu}$

is the wavenumber of emission and absorption,  $\epsilon$  is the dielectric constant, and  $n$  is the refractive index. A plot of the Stokes' shift as well as of the quantum yield of emission  $\Phi$  in dependence of  $F$  is shown in Figure 4. While the emission properties of **1** and **2** do not show a clear trend with changing solvents, **3** shows an increase in Stokes' shift and a slight decrease in  $\Phi$  with increasing  $F$ . The photophysical properties of this compound in methanol depart from the linear trend observed for the other solvents and, to a smaller extent, **1** and **2** also seem to be more affected by this solvent. Methanol is the only solvent that can form hydrogen bonds with the carbonyl oxygen atoms of the compounds studied here, providing thus



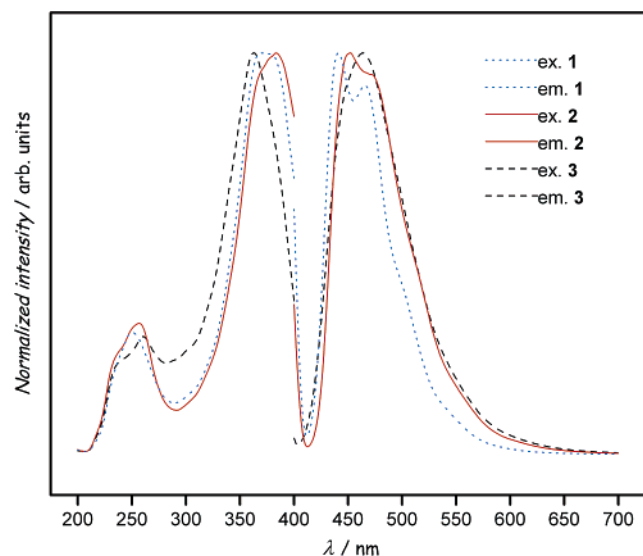


**Figure 3.** Normalized excitation and emission spectra of **1**, **2**, and **3** in methanol. Excitation spectra obtained with  $\lambda_{\text{em}} = \text{nm}$  and emission spectra obtained with  $\lambda_{\text{exc}} = \text{nm}$ . Excitation and emission slits were 5 nm and scan speed 500 nm/s.

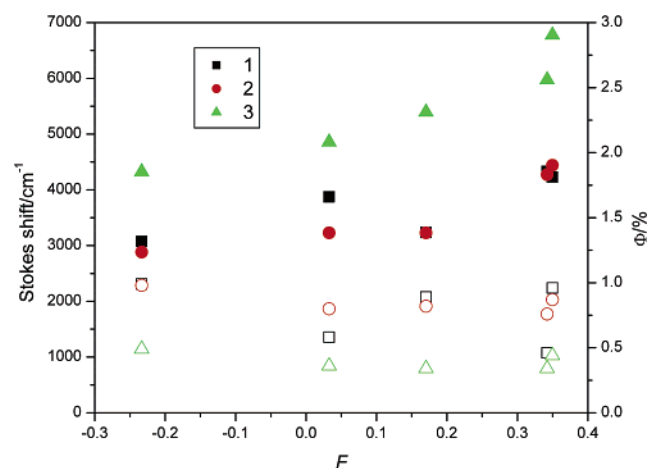


**Figure 4.** Dependence of the Stokes' shift (taken as the difference of the peak maxima; solid symbols) and the fluorescence quantum yield  $\Phi$  (open symbols) on  $F$  for **1** (squares), **2** (circles), and **3** (triangles).

strong short-range interactions, as mentioned above. Hydrogen-bonding interactions are also likely to be present between the solvent and the nitrogen atoms of the pyridine rings, as Mataga et al. observed.<sup>51</sup> Melhuish also observed an increase in emission efficiency in ethanol with respect to benzene and petroleum ether for fluorophores such as anthracene, perylene, anthranilic acid, and methyl anthranilate. The latter have hydrogen-bonding capability with the solvent, although an explanation of the solvent dependence was not given by the author.<sup>52</sup> A strong influence of hydrogen bonding on the emission behavior was also seen by Jarzaba and co-workers, who studied the solvatochromic shift of the emission of Coumarin 153 with solvent polarity in toluene–acetonitrile and toluene–methanol mixtures.<sup>53</sup> These authors saw, however, lower emission quantum yields in methanol as compared to acetonitrile, while we see the opposite.

The solid-state emission of these compounds was also investigated for the compounds and is summarized in Table 2. The spectra of the samples, dispersed in poly(methyl methacrylate) (PMMA) utilizing sodium salicylate (NaSal) in PMMA ( $\lambda_{\text{exc}} = 340 \text{ nm}$ ),<sup>54</sup> anthracene in PMMA ( $\lambda_{\text{exc}} = 366 \text{ nm}$ ),<sup>55</sup> and perylene in PMMA ( $\lambda_{\text{exc}} = 313 \text{ nm}$ )<sup>55</sup> as emission standards,

**TABLE 2: Photophysical Properties of Solids **1** through **3** in PMMA (~0.4–0.7% w/w)**

	<b>1</b>	<b>2</b>	<b>3</b>
$\lambda_{\text{em}}/\text{nm}$	540	585	584
$\Phi^a/\%$	$29 \pm 7$	$4 \pm 1$	$7 \pm 2$

<sup>a</sup> Measured at  $\lambda_{\text{exc}} = 313 \text{ nm}$  against perylene in PMMA,  $\Phi = 61\%$ ,<sup>55</sup> at  $\lambda_{\text{exc}} = 340 \text{ nm}$  against sodium salicylate in PMMA,  $\Phi = 53\%$ ,<sup>54</sup> and at  $\lambda_{\text{exc}} = 366 \text{ nm}$  against anthracene in PMMA,  $\Phi = 22\%$ .<sup>55</sup>

were measured utilizing a solid state holder in which the powders had a layer thickness of 2 mm or more, to prevent insufficient absorption of the exciting radiation. Lambertian emission behavior was assumed in all cases.<sup>54,56</sup> The wavelength of emission of all three compounds is strongly red-shifted with respect to the solution emission by up to 138 nm indicative of a certain degree of solid state aggregation and excimer emission, which is often seen in thiophene-based oligomers.<sup>57,58</sup> Solid-state quantum yields were determined to be 29% for **1**, 4% for **2**, and 7% for **3**. While **1** is clearly the stronger emitter in the solid state, the emission efficiencies of the other two compounds are similar within experimental error. The excimer emission shows that these three compounds display an appreciable degree of aggregation and therefore the inclusion of the phenylene moiety did not yield the hypsochromic shift that had been observed by Chan and co-workers who undertook a similar derivatization.<sup>34,59</sup> However, the emission efficiency of **1** is strong and, while measured dispersed in PMMA, comparable to other oligothiophenes such as the ones reported by Gigli and co-workers, which display solid-state quantum yields in the range 2% to 37%.<sup>33</sup> While the degree of efficiency was not reported, Hotta and co-workers also observed solid-state excimer emission for PTTP, with emission maxima of 530 and 560 nm, red-shifted by approximately 100 nm with respect to the solution behavior.<sup>36</sup>

**HOMO–LUMO Energies and Redox Behavior.** The determination of HOMO and LUMO energies allows matching the energies of charge carrier layers in LEDs. HOMO energies were measured by electrochemical methods and the HOMO–LUMO band gap was obtained through optical measurements from the onset of the absorption band. These values, along with the calculated ones, are summarized in Table 3. The HOMO energies determined to be in the range  $-5.93$  to  $-5.60 \text{ eV}$  and LUMO energies in the range  $-3.15$  to  $-2.90 \text{ eV}$  are comparable to other thiophene-based oligomers.<sup>60</sup> These values also agree well with the calculated HOMO and LUMO energies. For comparison, Katz and co-workers<sup>37</sup> reported the calculated HOMO energy of PTTP to be  $-5.16 \text{ eV}$  and the LUMO  $-1.69 \text{ eV}$ . Our HOMO energy is slightly lower, and it was reported that a stabilized HOMO can have a positive effect on materials to be utilized as semiconductors in organic field-effect transistors.<sup>37</sup>

The redox behavior of all three compounds was studied by cyclic voltammetry and the oxidation peak potentials are summarized in Table 3. These compounds are not reducible under the experimental conditions, but they all show well-defined and moderately reversible oxidation waves between 0.91 and 1.29 V vs  $\text{Ag}/\text{Ag}^+$ . While compounds **1** and **2** shown only one oxidation wave, **3** displays two quasireversible oxidation peaks. Due to the chemical, unsymmetrical nature of compound **3**, with its unsubstituted end-thiophene, the possibility of electrodimers exists. Thus, the cyclic voltammogram displays closely spaced oxidation waves. Two corresponding reduction peaks are seen in the reverse scan. As shown in Figure 5, upon repeated cycling all four original waves decrease in size and new oxidation waves grow in at  $\sim 0.7 \text{ V}$  and then at  $\sim 0.6$  and  $0.8 \text{ V}$ . In the reverse cycle peaks grow in at  $\sim 0.7$

TABLE 3: HOMO–LUMO Energies and  $E_{\text{ox}}$  of Compounds 1 through 3

compd	$E_{\text{ox}}/\text{V}^a$	$E_{\text{HOMO}}/\text{eV}^b$	$E_{\text{LUMO}}/\text{eV}^c$	$E_{\text{g}}/\text{eV}$	$E_{\text{HOMO}}/\text{eV}^d$	$E_{\text{LUMO}}/\text{eV}^d$	$E_{\text{g}}/\text{eV}^d$	dipole moment/ $\text{D}^d$
1	1.06	−5.62	−2.90	2.82	−5.55 (−5.61) <sup>e</sup>	−2.20 (−2.07) <sup>e</sup>	3.35 (3.54) <sup>e</sup>	
2	1.29	−5.93	−3.15	2.78	−5.77	−2.48	3.29	
3	0.91	−5.60	−2.69	2.91	−5.61	−2.20	3.41	3.5221

<sup>a</sup> Obtained by cyclic voltammetry in acetonitrile with 0.1 M TBAP vs Ag/Ag<sup>+</sup>. <sup>b</sup> Obtained by cyclic voltammetry from the onset of the oxidation wave. <sup>c</sup> Obtained from the onset of the absorption band by electron spectroscopy. <sup>d</sup> Obtained from DFT calculations (B3LYP/6-31G(d)). <sup>e</sup> Calculated from DFT without geometry optimization, with conformation obtained from X-ray data.

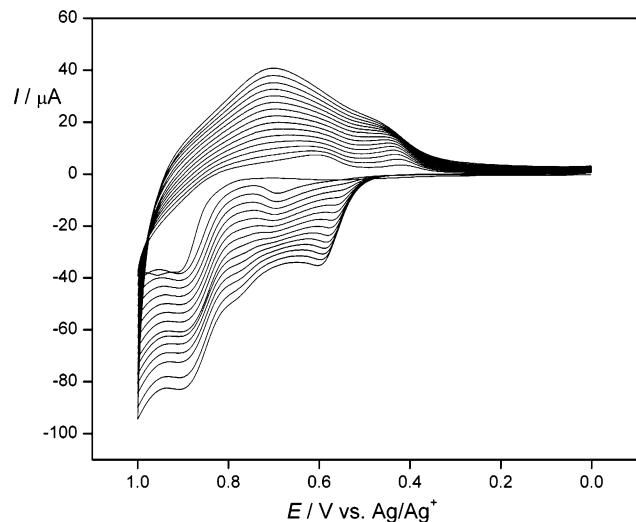


Figure 5. Cyclic voltammogram of 3, showing current increase upon repeated cycling; solution in acetonitrile with 0.1 M TBAP as supporting electrolyte; scan rate 100 mV/s.

and  $\sim 0.45$  V. This increase in current is accompanied by the deposition of a black coating on the electrode surface. We are currently studying the properties of the films deposited and their electrochemical properties and will report on them shortly.

## Conclusions

We have presented here three new compounds which show emission efficiencies of up to 99% in solution in the blue green region of the spectrum. In the solid state the emission, while still intense with quantum yield values of up to 29%, is in the green region of the spectrum, arising most likely from excimer emission. Compounds 1 and 2 show quasireversible oxidation in cyclic voltammetry experiments and electrochemical studies show that films utilizing 3 as the precursor can be electrodeposited. While the excimer emission observed in the solid state would allow their use only as moderately efficient green emitters, the HOMO energies determined experimentally and through calculations make these compounds possible candidates as organic semiconductors for field-effect transistor applications. The presence of the functional groups at the edges of the molecules allows for further derivatization and tailoring of system properties, as well as coordination to metal ions. These molecules can thus act as bridging ligands for transition metal ions for the formation of luminescent supramolecular frameworks or as sensitizers for lanthanide ion luminescence. Further, since 3 can be utilized in an electrodeposition process, this demonstrates the potential of electrochemical techniques as an alternative to spin-coating or vapor deposition of functional materials.

## Experimental Section

All commercially available reagents were used as received. Solvents were dried by standard methods. All reactions were

performed under nitrogen, using standard Schlenk technique. NMR spectra were recorded on a 300 MHz spectrometer. Indicated melting points are uncorrected. Experimental details on the spectroscopic measurements are included in the Supporting Information.

**Electrochemistry.** Cyclic voltammetry experiments were performed on a CHI 660A potentiometer with a standard three-electrode cell. The working electrode was a gold electrode 1 mm in diameter and the counter electrode a platinum wire, and a Ag/Ag<sup>+</sup> reference electrode (silver wire immersed in acetonitrile with 0.01 M AgNO<sub>3</sub> and 0.1 M tetrabutylammonium perchlorate (TBAP)) was used.

**Spectroscopy.** All solution measurements were performed at  $25.0 \pm 0.1$  °C, and solid state measurements were performed at  $20 \pm 2$  °C. Absorption and diffuse reflectance spectra were measured on a Perkin-Elmer Lambda35 spectrometer, equipped with a LabSphere diffuse reflectance accessory and a Spectralon standard for background correction. The emission spectra, corrected for instrumental response, were measured on a Perkin-Elmer LS-55 fluorescence spectrometer. For the emission and excitation spectra slit widths were 5 or 10 nm and scan rates of 250 nm/min were used. The quantum yields of emission in solution were determined against  $5 \times 10^{-6}$  M quinine sulfate in 0.1 N H<sub>2</sub>SO<sub>4</sub> ( $\Phi = 54.6\%$  at  $\lambda_{\text{exc}} = 366$  nm).<sup>61</sup> The samples for the solid-state quantum yield determination were finely ground with PMMA at a  $4 \times 10^{-3}$ – $7 \times 10^{-3}$  w/w concentration of the sample. The powders were deposited with a thickness of  $\sim 2$  mm onto the solid state holder. The solid-state quantum yields were determined against sodium salicylate NaSal ( $\Phi_{\text{ST}} = 53\%$  at  $\lambda_{\text{exc}} = 340$  nm<sup>54</sup>), perylene ( $\Phi_{\text{ST}} = 61\%$  at  $\lambda_{\text{exc}} = 313$  nm<sup>55</sup>), and anthracene ( $\Phi_{\text{ST}} = 22\%$  at  $\lambda_{\text{exc}} = 366$  nm<sup>55</sup>) in PMMA as described by Brill,<sup>62</sup> with  $\Phi_x = (1 - R_{\text{ST}})/(1 - R_x) \times (I_x/I_{\text{ST}}) \times \Phi_{\text{ST}}$ , where  $\Phi$  is the quantum yield,  $R$  the diffuse reflectance, and  $I$  the integrated emission spectrum of sample  $x$  and standard ST.  $R$  for sample  $x$  and standard ST were determined with the fluorimeter by scanning the emission monochromator through the excitation range and calibrating with the diffuse reflectance of PMMA. The diffuse reflectance of PMMA was determined to be  $R = 54.3\%$  at 313 nm, 59% at 340 nm, and 60% at 366 nm, with the diffuse reflectance accessory. Samples and standards were dissolved in PMMA to reduce self-absorbance of emitted light and to avoid refractive index corrections to the quantum yield.

**Synthesis: 1,4-Bis(2-thienyl)benzene (a).** This compound was synthesized according to a modified literature procedure:<sup>34</sup> A suspension of 1,4-dibromobenzene (3.50 g, 14.83 mmol), 2-thienylboronic acid (4.75 g, 37.01 mmol), K<sub>2</sub>CO<sub>3</sub> (10.5 g, 5 equiv), and Pd(PPh<sub>3</sub>)<sub>4</sub> (0.3 g, 2.61 mmol) in DMF (50 mL) was stirred overnight at 90 °C. The reaction mixture was cooled to room temperature, quenched with water (150 mL), and extracted with ether (200 mL). The organic layer was separated, and the aqueous layer was extracted with ether:EtOAc (150 mL, 1:1). The combined organic layers were washed with water ( $2 \times 50$  mL), dried over anhydrous MgSO<sub>4</sub>, and concentrated. The residue was recrystallized from EtOH:CHCl<sub>3</sub> 5:1 to provide 3.15

g (13.02 mmol, 88%) of the compound as slightly yellow powder.  $^1\text{H}$  NMR ( $\text{CDCl}_3$ )  $\delta$  7.64 (s, 4 H), 7.35 (dd,  $J$  = 3.6, 1.2 Hz, 2 H), 7.30 (dd,  $J$  = 5.1, 1.2 Hz, 2 H), 7.10 (m, 1 H).

**1,4-Bis(5-bromothiophen-2-yl)benzene (b).** This compound was synthesized according to a modified literature procedure:  $^{63}\text{NBS}$  (1.58 g, 8.47 mmol) was added in small portions to a stirred solution of 1,4-bis(2-thienyl)benzene (1.00 g, 4.13 mmol) in DMF (20 mL) at 0 °C in the dark. The resulting solution was stirred overnight at room temperature and then diluted with EtOH. A white precipitate formed which was filtered, washed with EtOH, and dried to provide 1.45 g (3.63 mmol, 88%) of 1,4-bis(5-bromothiophen-2-yl)benzene, which was not purified any further.

**1,4-Bis(5-tributyltinthiophen-2-yl)benzene (c).**  $n\text{-BuLi}$  (2.8 M in hexanes, 2.63 mmol, 0.93 mL) was added dropwise to a solution of crude **b** (0.50 g, 1.25 mmol) in anhydrous THF (20 mL) at  $-78$  °C, and the resulting mixture was stirred for 2 h at  $-78$  °C.  $\text{Bu}_3\text{SnCl}$  (0.85 g, 2.63 mmol) in THF (3 mL) was added at  $-78$  °C and the reaction vessel was slowly warmed to room temperature. The reaction mixture was stirred for 1 h at room temperature, poured into saturated  $\text{NH}_4\text{Cl}_{\text{aq}}$ , and extracted with ether. The combined organic extracts were washed with water and brine, dried over anhydrous  $\text{MgSO}_4$ , and concentrated. The residue was passed through a pad of alumina and used without further purification.

**1.** A solution of crude **c**, 4-bromopyridine-2,6-dicarboxylic acid bis(diethylamide), (0.91 g, 2.63 mmol), and  $\text{Pd}(\text{PPh}_3)_4$  (0.01 g, 0.09 mmol) in DMF (20 mL) was stirred overnight at 90–95 °C. The reaction was quenched with HCl (10%) and diluted with water and  $\text{CH}_2\text{Cl}_2$ . The organic layer was separated and the aqueous layer was extracted with  $\text{CH}_2\text{Cl}_2$  ( $2 \times 50$  mL). The combined organic extracts were washed with water ( $2 \times 30$  mL), dried over anhydrous  $\text{MgSO}_4$ , and concentrated. The residue was purified by flash chromatography over silica and gradual elution ( $\text{EtOAc}$ :petroleum ether: $\text{CH}_2\text{Cl}_2$  5:2:2 to  $\text{EtOAc}$ : $\text{CH}_2\text{Cl}_2$  1:1) to give 0.23 g (0.29 mmol, 23%) of **1**.  $^1\text{H}$  NMR ( $\text{CDCl}_3$ )  $\delta$  7.83 (s, 4 H), 7.69 (s, 4 H), 7.59 (d,  $J$  = 3.9 Hz, 2 H), 7.40 (d,  $J$  = 3.9 Hz), 3.60 (q,  $J$  = 7.2 Hz, 8 H), 3.40 (q,  $J$  = 6.9 Hz, 8 H), 1.30 (t,  $J$  = 7.2 Hz, 12 H), 1.19 (t,  $J$  = 6.9 Hz).  $^{13}\text{C}$  NMR ( $\text{CDCl}_3$ )  $\delta$  168.4, 155.0, 146.5, 143.7, 139.8, 133.8, 127.8, 126.8, 125.1, 119.7, 43.7, 40.6, 14.7, 13.2. Melting point 193 °C dec.

**2 and 3.** A solution of crude **c**, 4-bromo-pyridine-2,6-dicarboxylic acid diethylester (0.79 g, 2.63 mmol), and  $\text{Pd}(\text{PPh}_3)_4$  (0.01 g, 0.09 mmol) in DMF (20 mL) was stirred overnight at 90–95 °C. The reaction was quenched with HCl (10%) and diluted with water and  $\text{CH}_2\text{Cl}_2$ . The organic layer was separated and the aqueous layer was extracted with  $\text{CH}_2\text{Cl}_2$  ( $2 \times 50$  mL). The combined organic layers were washed with water ( $2 \times 30$  mL), dried over anhydrous  $\text{MgSO}_4$ , and concentrated. The residue was purified by flash chromatography over silica and gradual elution ( $\text{EtOAc}$ :petroleum ether: $\text{CH}_2\text{Cl}_2$  5:2:2 to  $\text{EtOAc}$ : $\text{CH}_2\text{Cl}_2$  1:1) to give 0.16 g (0.23 mmol, 19%) of **2** and 0.11 g (0.24 mmol, 19%) of **3** as yellow crystalline powders.

**2:**  $^1\text{H}$  NMR ( $\text{CDCl}_3$ )  $\delta$  8.46 (s, 4 H), 7.73 (s, 4 H), 7.70 (d,  $J$  = 3.9 Hz, 2 H), 7.45 (d,  $J$  = 3.9 Hz, 2 H), 4.53 (q,  $J$  = 7.2 Hz, 8 H), 1.50 (t,  $J$  = 7.2 Hz, 12 H).  $^{13}\text{C}$  NMR ( $\text{CDCl}_3$ )  $\delta$  164.9, 149.2, 146.8, 143.9, 138.7, 133.2, 128.0, 136.3, 124.9, 123.1, 62.9, 14.7. Melting point 295 °C dec.

**3:**  $^1\text{H}$  NMR ( $\text{CDCl}_3$ )  $\delta$  8.43 (s, 2 H), 7.67 (d,  $J$  = 3.9 Hz, 1 H), 7.65 (s, 4 H), 7.38 (d,  $J$  = 3.9 Hz), 7.36 (dd,  $J$  = 3.6, 1.2 Hz, 1 H), 7.31 (dd,  $J$  = 5.1, 1.2 Hz), 4.52 (q,  $J$  = 7.2 Hz, 4 H), 1.49 (t,  $J$  = 7.2 Hz, 6 H).  $^{13}\text{C}$  NMR ( $\text{CDCl}_3$ )  $\delta$  164.7, 149.3,

147.3, 143.8, 143.4, 138.1, 134.5, 132.2, 128.2, 127.9, 126.34, 126.28, 125.3, 124.5, 123.4, 123.0, 62.4, 14.2. Melting point 259 °C dec.

**Acknowledgment.** Syracuse University and the Petroleum Research Fund are gratefully acknowledged for financial support of this work.

**Supporting Information Available:** Selected bond lengths and angles for **1** as well as  $^1\text{H}$  NMR and  $^{13}\text{C}$  NMR spectra for compounds **a–e** and **1–3** and details of the X-ray diffraction experiment and calculations. This material is available free of charge via the Internet at <http://pubs.acs.org>.

## References and Notes

- (1) Tang, C. W.; VanSlyke, S. A. *Appl. Phys. Lett.* **1987**, *51* (12), 913–15.
- (2) Mueller, C. D.; Falcou, A.; Reckefuss, N.; Rojahn, M.; Wiederhirn, V.; Rudati, P.; Frohne, H.; Nuyken, O.; Becker, H.; Meerholz, K. *Nature* **2003**, *421* (6925), 829–833.
- (3) Nguyen, T.-P.; Molinier, P.; Destruel, P. Organic and polymer-based light-emitting diodes. In *Light-Emitting Diodes, Lithium Batteries, and Polymer Devices*; Nalwa, H. S., Ed.; Academic Press: New York, 2001; Vol. 10, pp 1–51.
- (4) Dai, L.; Winkler, B.; Dong, L.; Tong, L.; Mau, A. W. H. *Adv. Mater.* **2001**, *13*, (12–13), 915–925.
- (5) Kraft, A.; Grimsdale, A. C.; Holmes, A. B. *Angew. Chem., Int. Ed.* **1998**, *37* (4), 403–428.
- (6) Baldo, M. A.; Thompson, M. E.; Forrest, S. R. *Pure Appl. Chem.* **1999**, *71* (11), 2095–2106.
- (7) Meng, H.; Chen, Z.-K.; Huang, W. *J. Phys. Chem. B* **1999**, *103*, 6429.
- (8) Kim, Y.; Lee, J.-G.; Kim, S. *Adv. Mater.* **1999**, *11* (17), 1463–1466.
- (9) Lu, J.; Hlil, A. R.; Sun, Y.; Hay, A. S.; Maindrone, T.; Dodelet, J.-P.; D'Iorio, M. *Chem. Mater.* **1999**, *11* (9), 2501–2507.
- (10) Hu, N.-X.; Esteghamatian, M.; Xie, S.; Popovich, Z.; Hor, A.-M.; Ong, B.; Wang, S. *Adv. Mater.* **1999**, *11* (17), 1460–1463.
- (11) Hong, Z.; Li, W.; Zhao, D.; Liang, C.; Liu, X.; Peng, J.; Zhao, D. *Synth. Met.* **1999**, *104* (3), 165–168.
- (12) Wu, C. C.; Lin, Y. T.; Chiang, H. H.; Cho, T. Y.; Chen, C. W.; Wong, K. T.; Liao, Y. L.; Lee, G. H.; Peng, S. M. *Appl. Phys. Lett.* **2002**, *81* (4), 577–579.
- (13) Kinoshita, M.; Kita, H.; Shirota, Y. *Adv. Funct. Mater.* **2002**, *12* (11–12), 780–786.
- (14) Wang, B.-H.; Yin, J.; Xue, M. Z.; Wang, J. L.; Zhong, G.; Ding, X. *Synth. Met.* **2003**, *132* (2), 191–195.
- (15) Ma, D.; Wang, D.; Hong, Z.; Zhao, X.; Jing, X.; Wang, F. *Synth. Met.* **1997**, *91* (1–3), 331–332.
- (16) Huang, W.; Meng, H.; Yu, W.-L.; Gao, J.; Heeger, A. J. *Adv. Mater.* **1998**, *10* (8), 593–596.
- (17) Baumgarten, M.; Yuksel, T. *Phys. Chem. Chem. Phys.* **1999**, *1* (8), 1699–1706.
- (18) Kido, J.; Nagai, K.; Ohashi, Y. *Chem. Lett.* **1990**, 657–660.
- (19) Kido, J.; Nagai, K.; Okamoto, Y.; Skotheim, T. *Chem. Lett.* **1991**, 1267–1270.
- (20) Kido, J.; Okamoto, Y. *Chem. Rev.* **2002**, *102* (6), 2357–2368.
- (21) McGehee, M. D.; Bergstedt, T.; Zhang, C.; Saab, A. P.; O'Regan, M. B.; Bazan, G. C.; Srdanov, V. I.; Heeger, A. J. *Adv. Mater.* **1999**, *11* (16), 1349–1354.
- (22) Yu, G.; Liu, Y.; Wu, X.; Zhu, D.; Li, H.; Jin, L.; Wang, M. *Chem. Mater.* **2000**, *12* (9), 2537–2541.
- (23) Okada, K.; Wang, Y.-F.; Chen, T.-M.; Kitamura, M.; Nakaya, T.; Inoue, H. *J. Mater. Chem.* **1999**, *9* (12), 3023–3026.
- (24) Xin, H.; Sun, M.; Wang, K. Z.; Zhang, Y. A.; Jin, L. P.; Huang, C. H. *Chem. Phys. Lett.* **2004**, *388* (1–3), 55–57.
- (25) Huang, L.; Wang, K.-Z.; Huang, C.-H.; Li, F.-Y.; Huang, Y.-Y. *J. Mater. Chem.* **2001**, *11* (3), 790–793.
- (26) Guan, M.; Bian, Z. Q.; Li, F. Y.; Xin, H.; Huang, C. H. *New J. Chem.* **2003**, *27* (12), 1731–1734.
- (27) Bian, Z.; Gao, D.; Wang, K.; Jin, L.; Huang, C. *Thin Solid Films* **2004**, *460* (1–2), 237–241.
- (28) de Bettencourt-Dias, A. *Inorg. Chem.* **2005**, *44*, 2734–2741.
- (29) de Bettencourt-Dias, A.; Viswanathan, S.; Ruddy, K. *Cryst. Growth Des.* **2005**, *5*, 1477–1484.
- (30) Zechmeister, L.; Sease, J. W. *J. Am. Chem. Soc.* **1947**, *69*, 273–5.
- (31) Barbarella, G.; Melucci, M.; Sotgiu, G. *Adv. Mater.* **2005**, *17* (13), 1581–1593.



- (32) Barbarella, G.; Zambianchi, M.; Antolini, L.; Ostojia, P.; Maccagnani, P.; Bongini, A.; Marseglia, E. A.; Tedesco, E.; Gigli, G.; Cingolani, R. *J. Am. Chem. Soc.* **1999**, *121* (38), 8920–8926.
- (33) Gigli, G.; Barbarella, G.; Favaretto, L.; Cacialli, F.; Cingolani, R. *Appl. Phys. Lett.* **1999**, *75* (4), 439–441.
- (34) Xu, J.; Ng, S. C.; Chan, H. S. O. *Bull. Chem. Soc. Jpn.* **2003**, *76* (7), 1449–1458.
- (35) Hotta, S.; Kimura, H.; Lee, S. A.; Tamaki, T. *J. Heterocycl. Chem.* **2000**, *37* (2), 281–286.
- (36) Lee, S. A.; Hotta, S.; Nakanishi, F. *J. Phys. Chem. A* **2000**, *104* (9), 1827–1833.
- (37) Hong, X. M.; Katz, H. E.; Lovinger, A. J.; Wang, B.-C.; Raghavachari, K. *Chem. Mater.* **2001**, *13* (12), 4686–4691.
- (38) de Bettencourt-Dias, A.; Viswanathan, S. *Chem. Commun.* **2004**, 1024–1025.
- (39) Zheng, Z.; Wang, J.; Liu, H.; Carducci, M. D.; Peyghambarian, N.; Jabbour, G. E. *Acta Cryst. C* **2002**, *C58* (1), m50–m52.
- (40) Fichou, D. *J. Mater. Chem.* **2000**, *10* (3), 571–588.
- (41) Katz, H. E. *J. Mater. Chem.* **1997**, *7* (3), 369–376.
- (42) Pouzet, P.; Erdelmeier, I.; Ginderow, D.; Mornon, J.-P.; Dansette, P. M.; Mansuy, D. *J. Heterocycl. Chem.* **1997**, *34* (5), 1567–1574.
- (43) Ando, S.; Ueda, M. *Synth. Met.* **2002**, *129* (2), 207–213.
- (44) De Oliveira, M. A.; Dos Santos, H. F.; De Almeida, W. B. *Phys. Chem. Chem. Phys.* **2000**, *2* (15), 3373–3380.
- (45) Desiraju, G. R. *Chem. Commun.* **2005**, (24), 2995–3001.
- (46) Shah, B. K.; Neckers, D. C.; Shi, J.; Forsythe, E. W.; Morton, D. *Chem. Mater.* **2006**, *18* (3), 603–608.
- (47) Jia, W. L.; Feng, X. D.; Bai, D. R.; Lu, Z. H.; Wang, S.; Vamvounis, G. *Chem. Mater.* **2005**, *17* (1), 164–170.
- (48) Murase, T.; Fujita, M. *J. Org. Chem.* **2005**, *70* (23), 9269–9278.
- (49) Lippert, E. *Acc. Chem. Res.* **1970**, *3* (2), 74–80.
- (50) Mataga, N.; Kaifu, Y.; Koizumi, M. *Bull. Chem. Soc. Jpn.* **1956**, *29*, 465–70.
- (51) Mataga, N.; Tsuno, S. *Bull. Chem. Soc. Jpn.* **1957**, *30*, 368–74.
- (52) Melhuish, W. H. *J. Phys. Chem.* **1961**, *65*, 229–35.
- (53) Krolicki, R.; Jarzeba, W.; Mostafavi, M.; Lampre, I. *J. Phys. Chem. A* **2002**, *106* (9), 1708–1713.
- (54) Wrighton, M. S.; Ginley, D. S.; Morse, D. L. *J. Phys. Chem.* **1974**, *78* (22), 2229–33.
- (55) Melhuish, W. H. *J. Opt. Soc. Am.* **1964**, *54*, 183–6.
- (56) Allison, R.; Burns, J.; Tuzzolino, A. J. *J. Opt. Soc. Am.* **1964**, *54* (6), 747–51.
- (57) Löwe, C.; Weder, C. *Adv. Mater.* **2002**, *14* (22), 1625–1629.
- (58) Jaramillo-Isaza, F.; Turner, M. L. *J. Mater. Chem.* **2006**, *16* (1), 83–89.
- (59) Xu, J. M.; Ng, S. C.; Chan, H. S. O. *Macromolecules* **2001**, *34* (13), 4314–4323.
- (60) Perepichka, I. I.; Perepichka, I. F.; Bryce, M. R.; Palsson, L.-O. *Chem. Commun.* **2005**, (27), 3397–3399.
- (61) Zucchi, G.; Scopelliti, R.; Bünzli, J.-C. G. *Dalton Trans.* **2001**, (13), 1975–1985.
- (62) Bril, A.; De Jager-Veenis, A. W. *J. Res. Natl. Bur. Stand., Sect. A* **1976**, *80A* (3), 401–7.
- (63) Hotta, S.; Katagiri, T. *J. Heterocycl. Chem.* **2003**, *40* (5), 845–850.